

Elasto-plastic description of brittle failure in amorphous materials

Marko Popović, Tom W. J. de Geus, and Matthieu Wyart

Institute of Theoretical Physics, École Polytechnique Fédérale de Lausanne (EPFL), CH-1015 Lausanne, Switzerland

The response of amorphous materials to an applied strain can be continuous, or instead display a macroscopic stress drop when a shear band nucleates. Such discontinuous response can be observed if the initial configuration is very stable. We study theoretically how such brittleness emerges in athermal, quasi-statically driven, materials as their initial stability is increased. We show that this emergence is well reproduced by elasto-plastic models and is predicted by a mean field approximation, where it corresponds to a continuous transition. In mean field, failure can be forecasted from the avalanche statistics. We show that this is not the case for very brittle materials in finite dimensions due to rare weak regions where a shear band nucleates. Their critical radius is predicted to follow $a_c \sim (\Sigma - \Sigma_b)^{-2}$, where Σ is the stress and Σ_b the stress a shear band can carry.

How amorphous solids such as granular materials, bulk metallic glasses, colloidal suspensions or foams yield under an applied strain is a central question in fields as diverse as geophysics [1], material science [2] and soft matter [3]. At a macroscopic level, the stress *vs* strain curve under quasi-static loading can monotonically increase or slightly overshoot as in foams and granular materials [4] or even be discontinuous as in some metallic glasses [5]. This brittleness can have a catastrophic consequence, and appears to depend on a variety of factors including composition [6], Poisson’s ratio [6], temperature [7] and system preparation [8]. Spatially, it corresponds to the emergence of a shear band a few nanometers thick [9] where most of the strain localizes. Understanding what aspects of the material ultimately control brittleness and how shear bands nucleate remains a challenge. At a microscopic level, plasticity takes place by discrete events, the so-called shear transformations where a few particles rearrange locally [10–13]. The stress change it induces is anisotropic and long-range [13, 14], and can in turn trigger new plastic events, generating anisotropic avalanches of plasticity [15, 16]. It has been argued that amorphous solids are critical: plasticity in the solid phase occurs via avalanches that can be system spanning [17–19]. Yet it is unclear if these avalanches of plasticity are precursors of brittle failure [20, 21].

Recently, novel algorithms have been able to generate very stable glasses that are brittle. This previously impossible feat was achieved by obtaining quench rates comparable to experiments [22, 23] using swap algorithms [24, 25], or by shearing the system back and forth many times [26]. These studies underline the critical role of the system preparation in controlling brittleness. Theoretically, it was recently proposed that the yielding transition is a spinodal decomposition [27, 28], which occurs for example in a magnet if a field is applied in the direction opposed to its magnetization. The magnetization can evolve smoothly (“ductile” behavior) or rather suddenly (“brittle” behavior) depending on the amount of disorder [29, 30]. This analogy nicely explains why increasing the initial stability of the glass can lead to a ductile to brittle transition [22]. Yet, it does not incorporate the anisotropy of the interaction between shear transforma-

tions that causes shear bands, nor the criticality of the solid phase.

In this Letter, we first show that this ductile to brittle transition is well captured by elasto-plastic models [13] by increasing the stability of the initial configurations. We explain this observation in a mean field approximation where the transition is found to be continuous, and failure can indeed be anticipated from the distribution of avalanches. We then argue that these results break down for very stable glasses due to rare locations in the sample where a shear band nucleates: failure occurs if the spatial extension a of a weak region in the sample exceeds $a_c \sim (\Sigma - \Sigma_b)^{-2}$, where Σ is the stress and Σ_b is the stress that a shear band can carry. We confirm these results in elasto-plastic models, both by measuring the effect of inserting a weak “scar” in the material and by studying finite size effects. Overall, the framework we propose for how amorphous solids yield in quasi-static athermal conditions ties together ductile and brittle behavior, avalanche statistics and shear band nucleation of very brittle materials.

Brittleness in elasto-plastic models In elasto-plastic models [13, 31, 32] the material is divided into N elements, each characterized by its shear stress σ_i and yield stress σ_i^Y . The overall stress of the system is simply $\Sigma = \sum_i \sigma_i/N$. When $|\sigma_i|$ reaches σ_i^Y , the element yields: after a time τ its stress decreases by a value $\delta\sigma_i$, corresponding to a plastic deformation $\delta\epsilon_{p,i} = \delta\sigma_i/\mu_0$, where μ_0 is the shear modulus. New random variables σ_i and σ_i^Y are then taken from some distributions $P(\sigma)$ and $P_Y(\sigma^Y)$. Such a plastic event affects the stress everywhere in the material, according to a propagator $G(\vec{r})$ whose sign varies in space and which decays in magnitude as a dipole [13, 32, 33]. The specific parameters we use are described in the Supplementary Material. Such models have a finite macroscopic yield stress Σ_c so that the material is solid for $|\Sigma| < \Sigma_c$ and liquid for $|\Sigma| > \Sigma_c$ [13]. In the solid case these models predict how Σ depends on the accumulated plastic strain $\epsilon_p = \sum_i \epsilon_{p,i}/N$.

As the stress Σ is increased, most elements yield by reaching $\sigma_i = +\sigma_i^Y$. Therefore, it is useful to characterize elements by their stability $x_i = \sigma_i^Y - \sigma_i$. Depending on the initial distribution of stability $P_0(x)$, the stress was

found to overshoot or not [17, 34]. However, a brittle behavior has not been reported within these models.

We proceed by increasing stability of the distribution $P_0(x)$ as illustrated in Fig. 1a. For weakly stable initial states (case 1), the strain is homogeneous and the stress does not overshoot. When the initial stability is increased (case 2 in Fig. 1) the stress *vs* strain curve does display an overshoot. Although there is no macroscopic drop of stress, avalanches tend to localize along a rather thin shear band, as justified in [35, 36].

A key observation is that for very stable systems, the scenario changes: the stress *vs* strain curve becomes discontinuous (case 3 in Fig. 1). A very narrow shear band appears in one single avalanche, and relaxes the stress by some finite amount which persists in the thermodynamic limit, see below. This result supports that macroscopic failure can occur even in the absence of inertia and thermal feedback (in which strain increases temperature locally, which in turn localizes strain further), as these effects are absent in our model.

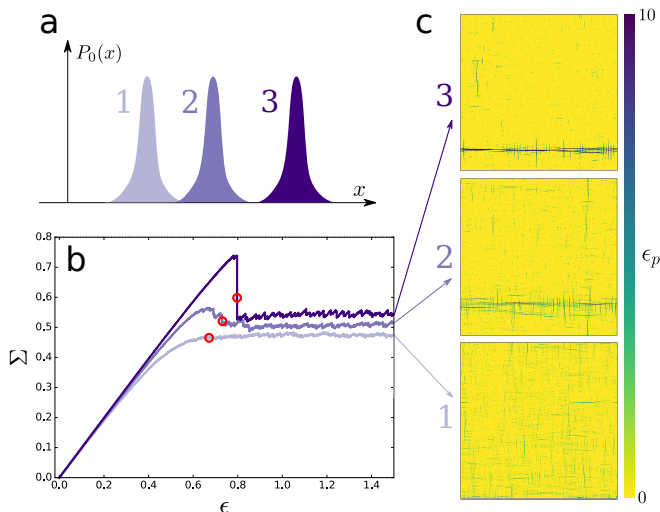


FIG. 1: An elasto-plastic model can be ductile without (1) and with (2) a stress overshoot, or brittle (3), depending on the preparation. a) Schematic of the initial distribution of stabilities, $P_0(x)$, representing the three system preparations. b) Stress strains curves for these three different $P_0(x)$ together with snapshots of the spatial distribution of plastic strain. c) 1: If the system is preparation is not very stable it will shear homogeneously and there will be no stress overshoot. 2: As the stability of preparation is increased a shear band is formed. 3: For a very stable preparation, a sharp shear band is formed during the brittle failure. Snapshots of the plastic strain are taken at positions indicated by red circles on stress *vs* strain curve.

Avalanches and macroscopic failure To explain this finding, we first consider the relationship between the avalanche size $S \equiv N\Delta\epsilon_p$, where $\Delta\epsilon_p$ is the total plastic strain accumulated during the avalanche, and the stress *vs* strain curve. When elements in the system begin to fail and the system deforms plastically, $P(x)$ develops a pseudo-gap $P(x) \sim x^\theta$ with $\theta > 0$ [37, 38]. This result

implies in turn that the minimal stability in the entire system (characterizing the size of the elastic ramps in Fig. 2a) follows $x_{min} \sim N^{-1/(1+\theta)}$ [39], which was shown to constrain avalanche statistics for stress-controlled loading [17].

We generalize this result by noting that controlling stress is a special case of a more general loading protocol in which a spring of elasticity μ_S is placed between the system and a strain controlled loading apparatus. Stress controlled loading then corresponds to $\mu_S \rightarrow 0$ and strain controlled loading to $\mu_S \rightarrow \infty$. The overall shear elastic constant of this combined system is $\mu = \mu_0\mu_S/(\mu_0 + \mu_S)$, equivalent to a serial connection of two springs with elastic constants μ_0 and μ_S . In practice, μ_S has a finite value, and experimental protocols lie between these limits. Consider an increment of stress $\Delta\Sigma = x_{min}$ followed by an avalanche where the stress drops by $\Delta\Sigma_{avalanche} = -\mu\Delta\epsilon_p$, which appears as a kink highlighted by the three black points in Fig. 2a. Requiring that on average this kink has an overall slope $\partial\Sigma/\partial\epsilon_p$, and using the definition of S as well as the scaling for x_{min} it follows that

$$\langle S \rangle \sim \frac{N^{\frac{\theta}{\theta+1}}}{1 + \frac{1}{\mu} \frac{\partial\Sigma}{\partial\epsilon_p}} \quad (1)$$

Key consequences of Eq. (1) are (i) $\partial\Sigma/\partial\epsilon_p = -\mu$ is a sufficient condition for macroscopic failure (not always necessary, see below). Thus, if the spring μ_S is stiff, macroscopic failure is less likely: in particular if $\min_{\epsilon_p} \partial\Sigma/\partial\epsilon_p > -\mu$ we predict no macroscopic failure. (ii) The mean avalanche size generically diverges with N , signaling crackling noise and system spanning avalanches even away from failure. This result is qualitatively different from disordered magnets [29] where the approach of failure is required for crackling to occur. However, the denominator in (1) diverges as the criterion $\partial\Sigma/\partial\epsilon_p \rightarrow -\mu$ is approached, suggesting that failure may be anticipated by monitoring avalanches.

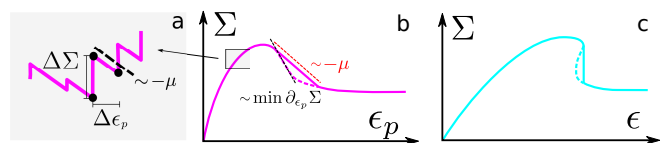


FIG. 2: a) Stress *vs* plastic strain curve consists of alternating elastic stress increases $\Delta\Sigma$ and stress relaxations by an avalanche of plastic events $\Delta\Sigma_{avalanche} = -\mu\Delta\epsilon_p$. b) When the slope of the macroscopic stress *vs* plastic strain curve reaches $-\mu$ an extensive avalanche occurs. c) Stress *vs* strain curve corresponding to the stress *vs* plastic strain curve from b) during a strain controlled loading.

Henceforth we shall focus on the strain controlled setup, where Eq. (1) becomes $\langle S \rangle \sim N^{\frac{\theta}{\theta+1}} (1 - (\partial\Sigma/\partial\epsilon)/\mu)$ where ϵ is the total strain $d\epsilon = d\epsilon_p + d\Sigma/\mu$. Then a sufficient condition for failure is that the stress *vs* strain curve develops an infinite slope, as illustrated in Fig. 2c.

Interestingly, it is still possible to probe this curve when it overhangs, if we allow the set-up to have a negative stiffness $\mu_S < 0$, as is the case in the formalism we now develop.

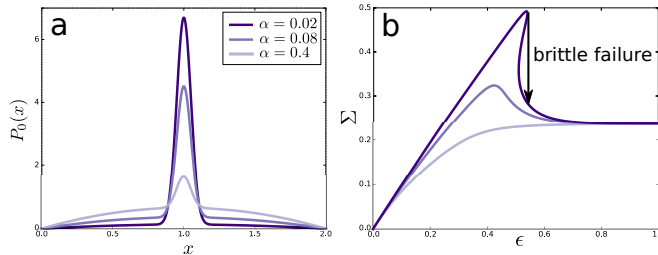


FIG. 3: a) Initial stability distributions $P_0(x) \sim (1 - \alpha) \exp(-(x-1)^2/(2s_P^2)) + \alpha x(2-x)$ with $s_P = 0.05$ we use to find b) stress vs strain curves in the Hebraud-Lequeux model, showing the ductile to brittle transition as the initial stability distribution $P_0(x)$ is narrowed.

Mean field approximation Following the previous paragraph, brittleness can be predicted by computing $\partial\Sigma/\partial\epsilon_p$. This is very hard in general because the mechanical noise generated by shear transformations is highly correlated in space. Mean field approximations neglect these correlations [40]. In its simplest form, the mechanical noise is assumed to be white, corresponding to the Hebraud-Lequeux model [40]. In more realistic mean field models, the noise is much broader, which leads to better values for the pseudo-gap exponent θ [38]. For our present purpose, however, we expect, and have checked numerically, that the two models lead to qualitatively similar behavior. We thus consider the simpler Hebraud-Lequeux model.

For simplicity, we assume yield stresses to be identical for all elements, and set its value σ^Y to unity. We further assume that locally the material is fully plastic, so that $\sigma_i \rightarrow 0$ and $x_i \rightarrow 1$ once element i yields. Thus $x_i = 0$ and $x_i = 2$ corresponds to the limit of stability of elements and elements that have yielded are reintroduced at $x_i = 1$. With this notation, the total stress is $\Sigma = 1 - \int_0^2 xP(x)dx$. The dynamical equation for the stability distribution $P(x)$ is a diffusion equation [40]

$$\partial_\gamma P(x, \gamma) = D\partial_x^2 P(x, \gamma) + v\partial_x P(x, \gamma) + \delta(x-1) \quad . \quad (2)$$

Here, $\gamma \equiv \epsilon_p \mu / \sigma^Y$ is number of plastic events per element, D characterizes the amplitude of the mechanical noise, and the source term describes the reinsertion of elements that have yielded. The drift v is a Lagrange multiplier that allows us to impose quasi-static loading. It is prescribed as follows: during quasi-static loading no elements are unstable in the thermodynamic limit, implying the boundary conditions $P(0) = P(2) = 0$. This condition precludes failure, which will instead be signaled by an overhanging stress vs strain curve. By integrating Eq. (2) we find that $\partial_x P(2, \gamma) - \partial_x P(0, \gamma) = -1/D$. In practice, the first term becomes very small as soon as the stress rises [38] because almost no sites yield in

the “wrong” direction at $x = 2$. Therefore, we can neglect the first term so that $\partial_x P(0, \gamma) = 1/D$. Taking the derivative of the stress, we now find

$$\partial_\gamma \Sigma = -1 + v = -1 - D^2 \partial_x^2 P(0, \gamma) \quad , \quad (3)$$

where we evaluated Eq. (2) at $x = 0$ to find $v = -D\partial_x^2 P(0, \gamma)/\partial_x P(0, \gamma)$. Using Eqs. (2) and (3), $P(x)$ can be computed for any given $P_0(x)$, allowing us to compute $\Sigma(\gamma)$ from Eq. (3).

We demonstrate the existence of a ductile to brittle transition using initial stability distribution $P_0(x) \sim (1 - \alpha) \exp(-(x-1)^2/(2s_P^2)) + \alpha x(2-x)$, where $s_P = 0.05$ is kept constant and the distribution is normalized to 1 on the interval $x \in [0, 2]$, as shown in Fig. 3a. For $\alpha = 0.4$ the stress does not overshoot while for $\alpha = 0.02$ the system is brittle. At an intermediate value $\alpha = 0.08$ the system is still ductile but the stress overshoots, as shown in Fig. 3b. Since $P_0(x)$ changes smoothly with α there has to be an α_c at which brittle failure occurs. This transition is continuous and of the usual saddle-node type, so that the magnitude of the stress jump scales as $\Delta\Sigma \sim (\alpha_c - \alpha)^{1/2}$. The same exponents are found in mean field disordered magnets [22, 30]. However, avalanches behave differently than in magnets: from Eq. (1) and the smoothness of the $\Sigma(\epsilon)$ curve, we get for brittle materials that $\langle S \rangle \sim \sqrt{N}/\sqrt{\epsilon_c - \epsilon}$ where ϵ_c is the strain at which failure occurs. Avalanches statistics can thus be used to forecast ϵ_c .

Our results have an interesting microscopic interpretation in terms of avalanches: from Eqs.(1) and (3) we obtain that $\langle S \rangle \sim -\sqrt{N}/\partial_x^2 P(0)$ for $\partial_x^2 P(0) < 0$ and it diverges otherwise. The avalanche size is thus controlled by the curvature of $P(x)$ at $x = 0$, whereby brittle failure occurs when this curvature vanishes. This result can be rationalized by a simple scaling argument following ideas from [41]. When an avalanche is initiated, the instantaneous number of unstable elements n_u evolves at each plastic event, and the avalanche ends when n_u returns to 0. If $P(x) = x/D$, during each plastic event one element is stabilized and on average one element becomes unstable. Therefore, n_u performs a simple random walk and there is no cutoff S_c in the avalanche size distribution. However, if the quadratic term is finite $P(x) = x/D + \partial_x^2 P(0)x^2/2$ and a drift appears in the evolution of n_u . When $\partial_x^2 P(0) < 0$, on average less than one element becomes unstable per plastic event and the drift is negative. S_c corresponds to the avalanche size where the integrated drift $-N \int_0^{x_c} \partial_x^2 P(0)x^2 dx$ is of the order of fluctuations $S_c^{1/2}$. Here, $x_c \sim \sqrt{2DS_c/N}$ is the characteristic value of the initial stability of elements that became unstable in the avalanche. We thus obtain $S_c \sim -N^{1/2}/\partial_x^2 P(0)$: the negative curvature of $P(x)$ at $x = 0$ determines the avalanche size by depleting the pool of elements that can become unstable.

Nucleation of shear band We now argue that for very brittle materials at least, macroscopic failure can occur without the apparent divergence of avalanche size described by Eq. (1); and thus cannot be easily anticipated

by a growing crackling noise. Instead, a shear band can nucleate in a region which, by chance, is weaker than the rest of the material. Consider a region of dimension $d - 1$, where d is the spatial dimension, and of linear extension a that has already yielded, and thus has smaller yield stresses than the rest of the material. We denote by Σ_b the shear stress such a narrow shear band can sustain in the limit of large a (Σ_b can in general depend on system preparation). If $\Sigma > \Sigma_b$, the stress will be distorted by this weak region. This is a classical calculation of fracture mechanics [42], leading to a stress at a distance r to the tip of the shear band of order $\Sigma(r) \sim (\Sigma - \Sigma_b)\sqrt{a}/\sqrt{r} \equiv \mathcal{K}/\sqrt{r}$ where \mathcal{K} is called the intensity factor. In analogy with fracture mechanics, we expect the shear band to propagate if \mathcal{K} is larger than

some critical value \mathcal{K}_c , leading to a critical nucleus size a_c triggering failure:

$$a_c \sim \frac{1}{(\Sigma - \Sigma_b)^2} \quad (4)$$

Eq. (4) is easily tested in elasto-plastic models by inserting a “scar”, i.e. a region with unusually small yield stresses of extension a_s . This procedure is analogous to the introduction of a void in a material, as is often used to measure its fracture toughness [42]. From Eq. (4) we expect a brittle failure to occur for some Σ_{\max} satisfying $\Sigma_{\max} - \Sigma_b \sim 1/\sqrt{a_s}$. This prediction is confirmed in Fig. 4a,b.

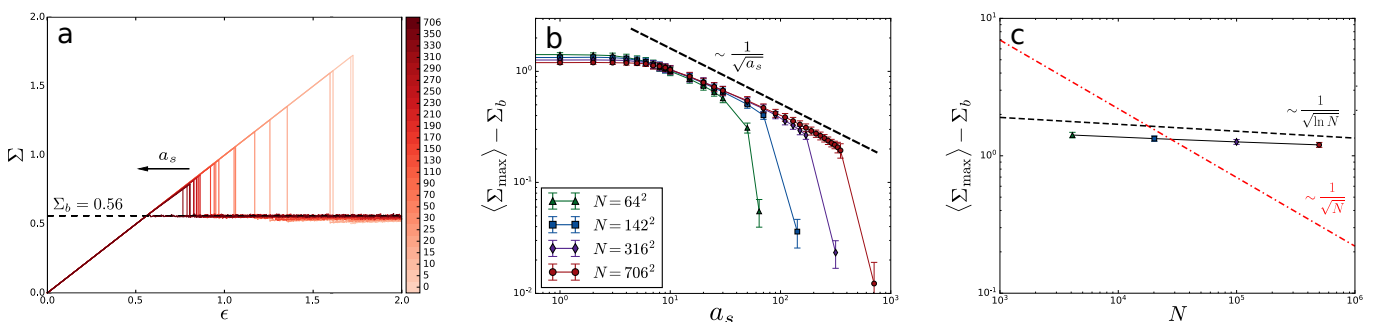


FIG. 4: a) Stress *vs* strain curve in an elasto-plastic model with $N = 706^2$ in which a scar of varying size a_s (as indicated in color) was inserted. b) Maximal stress reached Σ_{\max} as a function of the scar length a_s . c) When no scars are inserted, Σ_{\max} decreases very slowly with N , consistent with our prediction $\Sigma_{\max} - \Sigma_b \sim 1/\sqrt{\ln N}$.

In a large, homogeneously prepared system, spontaneous shear bands will occur. The probability to find a weak region of spatial extension a follows $p(a) \sim N \exp(-a^{d-1})$, the largest weak region formed by chance follows $a \sim (\ln N)^{1/(d-1)}$. Together with Eq. (4) this leads to $\Sigma_{\max} - \Sigma_b \sim 1/(\ln N)^{1/(2(d-1))}$. This decay is so weak that even for N of the order of the Avogadro number, we expect the overshoot to be significant. It is hard to test this asymptotic result numerically. However we find that for the elasto-plastic model, the dependence of Σ_{\max} with N is consistent with the slow decay predicted, as shown in Fig. 4c. The data exclude the more rapid decay $1/\sqrt{N}$ expected from a naive central limit theorem argument.

Conclusion Brittleness is one of the most practically important properties of materials. We have shown that elasto-plastic models can reproduce the ductile to brittle transition in amorphous solids as their initial stability is increased, in agreement with experimental and recent numerical observations. We have explained this result in a mean field approximation, in which macroscopic failure can always be predicted by a growing crackling noise. We have argued, however, that for very brittle materials, failure is induced by rare events in which a shear band nucleates, which cannot be forecasted, and we have

provided a theoretical description of this nucleation.

Our work suggests interesting venues for further theoretical and experimental studies. Both the anatomy of the shear bands as well as the possibility that failure can be anticipated by crackling noise in some regimes could be investigated systematically in terms of relevant parameters, including system preparation, loading apparatus but also strain rate and temperature, which has recently been incorporated in elasto-plastic models [43].

Acknowledgments

We thank L. Berthier, G. Biroli, M. Ozawa, G. Tarjus and A. Rosso for sharing unpublished results and discussions and the Simons collaboration for discussions. M. W. thanks the Swiss National Science Foundation for support under Grant No. 200021-165509 and the Simons Foundation Grant (#454953 Matthieu Wyart). T. G. was partly financially supported by The Netherlands Organisation for Scientific Research (NWO) by a NWO Rubicon grant number 680-50-1520. We acknowledge open-source software: the SciPy ecosystem [44] and GNU parallel [45].

-
- [1] P.A. Johnson and X. Jia. Nonlinear dynamics, granular media and dynamic earthquake triggering. *Nature*, 437(7060):871–874, 2005. doi: 10.1038/nature04015.
- [2] J. Schroers and W.L. Johnson. Ductile Bulk Metallic Glass. *Phys. Rev. Lett.*, 93(25):255506, 2004. doi: 10.1103/PhysRevLett.93.255506.
- [3] D. Bonn, M.M. Denn, L. Berthier, T. Divoux, and S. Manneville. Yield stress materials in soft condensed matter. *Rev. Mod. Phys.*, 89(3):035005, 2017. doi: 10.1103/RevModPhys.89.035005. arXiv: 1502.05281.
- [4] B. Andreotti, Y. Forterre, and O. Pouliquen. *Granular media: between fluid and solid*. Cambridge University Press, 2013.
- [5] J. Antonaglia, X. Xie, G. Schwarz, M. Wraith, J. Qiao, Y. Zhang, P.K. Liaw, J.T. Uhl, and K.A. Dahmen. Tuned Critical Avalanche Scaling in Bulk Metallic Glasses. *Sci. Rep.*, 4(1):4382, 2015. doi: 10.1038/srep04382.
- [6] J.J. Lewandowski, W.H. Wang, and A.L. Greer. Intrinsic plasticity or brittleness of metallic glasses. *Philos. Mag. Lett.*, 85(2):77–87, 2005. doi: 10.1080/09500830500080474.
- [7] J. Lu, G. Ravichandran, and W.L. Johnson. Deformation behavior of the $Zr_{41.2}Ti_{13.8}Cu_{12.5}Ni_{10}Be_{22.5}$ bulk metallic glass over a wide range of strain-rates and temperatures. *Acta Mater.*, 51(12):3429–3443, 2003. doi: 10.1016/S1359-6454(03)00164-2.
- [8] X.J. Gu, S.J. Poon, G.J. Shiflet, and J.J. Lewandowski. Ductile-to-brittle transition in a Ti-based bulk metallic glass. *Scr. Mater.*, 60(11):1027–1030, 2009. doi: 10.1016/j.scriptamat.2009.02.037.
- [9] Y. Zhang and A.L. Greer. Thickness of shear bands in metallic glasses. *Appl. Phys. Lett.*, 89(7):071907, 2006. doi: 10.1063/1.2336598.
- [10] A.S. Argon. Plastic deformation in metallic glasses. *Acta Metall.*, 27(1):47–58, 1979. doi: 10.1016/0001-6160(79)90055-5.
- [11] M.L. Falk and J.S. Langer. Dynamics of viscoplastic deformation in amorphous solids. *Phys. Rev. E*, 57(6):7192–7205, 1998. doi: 10.1103/PhysRevE.57.7192.
- [12] P. Schall, D.A. Weitz, and F. Spaepen. Structural Rearrangements That Govern Flow in Colloidal Glasses. *Science*, 318(5858):1895–1899, 2007. doi: 10.1126/science.1149308.
- [13] A. Nicolas, E.E. Ferrero, K. Martens, and J.-L. Barrat. Deformation and flow of amorphous solids: a review of mesoscale elastoplastic models. *arXiv Prepr.*, 2017. arXiv: 1708.09194.
- [14] G. Picard, A. Ajdari, F. Lequeux, and L. Bocquet. Elastic consequences of a single plastic event: A step towards the microscopic modeling of the flow of yield stress fluids. *Eur. Phys. J. E*, 15(4):371–381, 2004. doi: 10.1140/epje/i2004-10054-8. arXiv: 46.25.Cc Theoretical studies,83.10.Ff Continuum mechanics,83.60.La Viscoplasticity,yield stress.
- [15] A. Lemaître and C. Caroli. Rate-Dependent Avalanche Size in Athermally Sheared Amorphous Solids. *Phys. Rev. Lett.*, 103(6):065501, 2009. doi: 10.1103/PhysRevLett.103.065501.
- [16] C.E. Maloney and M.O. Robbins. Anisotropic Power Law Strain Correlations in Sheared Amorphous 2D Solids. *Phys. Rev. Lett.*, 102(22):225502, 2009. doi: 10.1103/PhysRevLett.102.225502.
- [17] J. Lin, T. Gueudré, A. Rosso, and M. Wyart. Criticality in the Approach to Failure in Amorphous Solids. *Phys. Rev. Lett.*, 115(16):168001, 2015. doi: 10.1103/PhysRevLett.115.168001.
- [18] M. Müller and M. Wyart. Marginal Stability in Structural, Spin, and Electron Glasses. *Annu. Rev. Condens. Matter Phys.*, 6(1):177–200, 2015. doi: 10.1146/annurev-conmatphys-031214-014614.
- [19] Z. Budrikis, D.F. Castellanos, S. Sandfeld, M. Zaiser, and S. Zapperi. Universal features of amorphous plasticity. *Nat. Commun.*, 8:15928, 2017. doi: 10.1038/ncomms15928.
- [20] F. Gimbert, D. Amitrano, and J. Weiss. Crossover from quasi-static to dense flow regime in compressed frictional granular media. *EPL (Europhysics Lett.)*, 104(4):46001, 2013. doi: 10.1209/0295-5075/104/46001. arXiv: 1208.1930.
- [21] A. Le Bouil, A. Amon, S. McNamara, and J. Crasous. Emergence of Cooperativity in Plasticity of Soft Glassy Materials. *Phys. Rev. Lett.*, 112(24):246001, 2014. doi: 10.1103/PhysRevLett.112.246001.
- [22] L. Berthier, G. Biroli, M. Ozawa, G. Tarjus, and A. Rosso. *In Preparation*, 2018.
- [23] Y. Jin, P. Urbani, F. Zamponi, and H. Yoshino. A stability-reversibility map unifies elasticity, plasticity, yielding and jamming in hard sphere glasses. *arXiv Prepr.*, 2018. arXiv: 1803.04597.
- [24] A. Ninarello, L. Berthier, and D. Coslovich. Models and Algorithms for the Next Generation of Glass Transition Studies. *Phys. Rev. X*, 7(2):021039, 2017. doi: 10.1103/PhysRevX.7.021039. arXiv: 1704.08864.
- [25] C. Brito, E. Lerner, and M. Wyart. Theory for Swap Acceleration near the Glass and Jamming Transitions. *arXiv Prepr.*, 2018. arXiv: 1801.03796.
- [26] P. Leishangthem, A.D.S. Parmar, and S. Sastry. The yielding transition in amorphous solids under oscillatory shear deformation. *Nat. Commun.*, 8:14653, 2017. doi: 10.1038/ncomms14653.
- [27] C. Rainone, P. Urbani, H. Yoshino, and F. Zamponi. Following the Evolution of Hard Sphere Glasses in Infinite Dimensions under External Perturbations: Compression and Shear Strain. *Phys. Rev. Lett.*, 114(1):015701, 2015. doi: 10.1103/PhysRevLett.114.015701.
- [28] G. Parisi, I. Procaccia, C. Rainone, and M. Singh. Shear bands as manifestation of a criticality in yielding amorphous solids. *Proc. Natl. Acad. Sci.*, 114(22):5577–5582, 2017. doi: 10.1073/pnas.1700075114.
- [29] J.P. Sethna, K. Dahmen, S. Kartha, J.A. Krumhansl, B.W. Roberts, and J.D. Shore. Hysteresis and hierarchies: Dynamics of disorder-driven first-order phase transformations. *Phys. Rev. Lett.*, 70(21):3347–3350, 1993. doi: 10.1103/PhysRevLett.70.3347.
- [30] S.K. Nandi, G. Biroli, and G. Tarjus. Spinodals with Disorder: From Avalanches in Random Magnets to Glassy Dynamics. *Phys. Rev. Lett.*, 116(14):145701, 2016. doi: 10.1103/PhysRevLett.116.145701.
- [31] J.-C. Baret, D. Vandembroucq, and S. Roux. Extremal Model for Amorphous Media Plasticity. *Phys. Rev. Lett.*, 89(19):195506, 2002. doi: 10.1103/PhysRevLett.89.195506.

- [32] G. Picard, A. Ajdari, F. Lequeux, and L. Bocquet. Slow flows of yield stress fluids: Complex spatiotemporal behavior within a simple elastoplastic model. *Phys. Rev. E*, 71(1):010501, 2005. doi: 10.1103/PhysRevE.71.010501.
- [33] V. Démery, V. Dansereau, E. Berthier, L. Ponson, and J. Weiss. Elastic interactions in damage models of brittle failure. *arXiv Prepr.*, 2017. arXiv: 1712.08537.
- [34] E.A. Jagla. Strain localization driven by structural relaxation in sheared amorphous solids. *Phys. Rev. E*, 76(4):046119, 2007. doi: 10.1103/PhysRevE.76.046119.
- [35] M.L. Manning, J.S. Langer, and J.M. Carlson. Strain localization in a shear transformation zone model for amorphous solids. *Phys. Rev. E*, 76(5):056106, 2007. doi: 10.1103/PhysRevE.76.056106.
- [36] R.L. Moorcroft and S.M. Fielding. Criteria for Shear Banding in Time-Dependent Flows of Complex Fluids. *Phys. Rev. Lett.*, 110(8):086001, 2013. doi: 10.1103/PhysRevLett.110.086001.
- [37] J. Lin, A. Saade, E. Lerner, A. Rosso, and M. Wyart. On the density of shear transformations in amorphous solids. *EPL (Europhysics Lett.)*, 105(2):26003, 2014. doi: 10.1209/0295-5075/105/26003.
- [38] J. Lin and M. Wyart. Mean-Field Description of Plastic Flow in Amorphous Solids. *Phys. Rev. X*, 6(1):011005, 2016. doi: 10.1103/PhysRevX.6.011005.
- [39] S. Karmakar, E. Lerner, and I. Procaccia. Statistical physics of the yielding transition in amorphous solids. *Phys. Rev. E*, 82(5):055103, 2010. doi: 10.1103/PhysRevE.82.055103.
- [40] P. Hébraud and F. Lequeux. Mode-Coupling Theory for the Pasty Rheology of Soft Glassy Materials. *Phys. Rev. Lett.*, 81(14):2934–2937, 1998. doi: 10.1103/PhysRevLett.81.2934.
- [41] E.A. Jagla. Avalanche-size distributions in mean-field plastic yielding models. *Phys. Rev. E*, 92(4):042135, 2015. doi: 10.1103/PhysRevE.92.042135.
- [42] T.L. Anderson. *Fracture Mechanics, Fundamentals and Applications*. CRC Press, 3rd edition, 2005. ISBN 0-8493-1656-1.
- [43] C. Liu, K. Martens, and J.-L. Barrat. Mean-Field Scenario for the Athermal Creep Dynamics of Yield-Stress Fluids. *Phys. Rev. Lett.*, 120(2):028004, 2018. doi: 10.1103/PhysRevLett.120.028004.
- [44] E. Jones, T. Oliphant, P. Peterson, and Others. SciPy: Open source scientific tools for Python. URL <http://www.scipy.org/>.
- [45] O. Tange. GNU Parallel - The Command-Line Power Tool. *login USENIX Mag.*, 36(1):42–47, 2011. doi: 10.5281/zenodo.16303.

Supplementary Material of “Elasto-plastic description of brittle failure in amorphous materials”

I. IMPLEMENTATION OF THE ELASTO-PLASTIC MODEL

We implement a two-dimensional elasto-plastic model on a periodic lattice of sizes $L = 64, 142, 316, 706$. The propagator $G(r, \phi)$ is a periodic version of an infinite system propagator $G_0(r, \phi) \sim \cos 4\phi/r^2$ and it is normalized so that $G(\vec{r} = 0) = -1$. This propagator preserves the sum of stresses along each row and column of elements. Thus, to keep the sum of stresses in all rows and columns the same during the initialization of the stress distribution $P(\sigma)$ we proceed as follows. We start with 0 stress in each element. Then, for each element i we draw a random stress $\delta\sigma$ from a normal distribution $\mathcal{N}(0, s_0^2)$ and we draw two random integer numbers δx and δy between 1 and the system’s length L . Then we add the stress $\delta\sigma$ to element i and the element at coordinates $(x_i - \delta x, y_i - \delta y)$ and we subtract $\delta\sigma$ from the stresses of elements at positions $(x_i - \delta x, y_i)$ and $(x_i, y_i - \delta y)$. Periodicity is imposed when needed. Finally, since on average each element has received a stress update 4 times by a random number drawn from a normal distribution of variance s_0^2 , we divide the stress of all elements by 2 to keep the variance of the initial stress distribution equal to s_0^2 . We use $s_0 = 0.45$ in Fig. 1 and $s_0 = 0.3$ in Fig. 4.

The initial distribution of yield stresses $P(\sigma^Y)$ is a normal distribution $\mathcal{N}(m, 0.01)$. In cases 1, 2 and 3 in Fig. 1 we use $m = 1.3, 1.5, 1.8$. In Fig. 4 $m = 3.0$ except in the “scar” region where $m = 1.0$.

After a plastic failure, the yield stress of the element is updated with a random number from a normal distribution $\mathcal{N}(1, 0.01)$, and the stress of the element is set to a random value drawn from a normal distribution $\mathcal{N}(0, 0.01)$.